Proposal of Vibration Suppression and Disturbance Rejection Control in Semi-Nyquist Frequency Region Based on Multirate Sampling Control

Hiroshi Fujimoto* and Yoichi Hori (The University of Tokyo)

Abstract

In this paper, novel multirate feedback controllers are proposed for digital control systems, where it is restricted that the speed of the A/D converters are slower than that of the D/A converters. The proposed controllers achieve vibration suppression and disturbance rejection even in the semi-Nyquist frequency region. First, the continuous-time vibration suppression controller is exactly discretized by the multirate sampling control based on the closed-loop characteristics. Second, the multirate repetitive controllers are proposed both by the feedback and feedforward approaches. The proposed controllers are applied to the settling and following modes of hard disk drive, and the advantages of these approaches are demonstrated by simulations.

Keywords: multirate sampling control, vibration suppression, discretization of controller, disturbance rejection, repetitive control, hard disk drive

1 Introduction

A digital control system usually has two samplers for the reference signal $r(t)$ and the output $y(t)$, and one holder on the input $u(t)$ as shown in Fig.1. Therefore, there exist three time periods T_r, T_y, and T_u which represent the period of $r(t), y(t)$, and $u(t)$, respectively. The input period T_u is generally decided by the speed of the actuator, D/A converter, or the calculation on the CPU. Moreover, the output period T_y is also determined by the speed of the sensor or the A/D converter. Practical control systems usually hold the restrictions on T_u and/or T_y. Thus, the conventional digital control systems make these three periods equal to the longer period between T_u and T_y.

In this paper, the digital control systems with longer sampling period $(T_u < T_y)$ are considered. This restriction may be general because D/A converters are usually faster than the A/D converters. Especially, head-positioning systems of the hard disk drive (HDD) or the visual servo systems of robot manipulator belong to this category, because the sampling rates of the measurement are relatively slow.

For these systems, it is difficult to suppress vibration and to reject disturbance in high frequency region because the Nyquist frequency is relatively low. In this paper, multirate sampling control is introduced, in which the plant input is changed N times during one sampling period. This scheme is also called the multirate input control. Using this scheme, novel multirate feedback controllers are proposed, which achieve vibration suppression and disturbance rejection even in the semi-Nyquist frequency region. Moreover, the proposed methods are applied to the head-positioning system of hard disk drive.

A vibration suppression controller is generally designed in the continuous-time system. To implement it in the digital control system, the designed analog controller is discretized by the Tustin transformation or other meth-
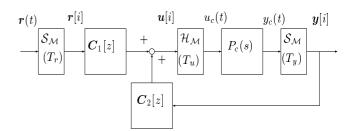

Fig. 1: Two-degree-of-freedom control system.

ods. Because these transformations are based only on the open-loop characteristics of the controller, the closed-loop becomes low performance or unstable when the control bandwidth is closed to the Nyquist frequency.

On the other hand, introducing multirate sampling control, the first author proposed a novel discretization method of controllers based on the closed-loop characteristics [1]. In this paper, this approach is extended to the hardware restricion of $(T_u < T_y)$ and applied to the vibration suppression controller. The advantages of the proposed method are that the controller is discretized based on the closed-loop characteristics, and the plant state of the digitally controlled system completely matches that of the original continuous-time system at M inter-sample points during T_y.

In the repetitive control system, conventional single-rate controllers do not have enough inter-sample performance to reject disturbance in the semi-Nyquist frequency region. On the other hand, authors proposed a novel multirate feedback controller, which achieves the perfect disturbance rejection at M inter-sample points [2]. In this paper, the proposed approach is modified to repetitive control, and applied to reject high order repeatable runout of hard disk drive.

Repetitive feedback controllers based on the internal model principle have disadvantages that the closed-loop
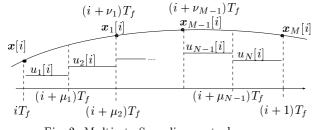
Fig. 2: Multirate Sampling control.

characteristics become worse and difficult to assure stability robustness [3]. Therefore, this paper proposes novel approach which never has these problems, based on the open-loop estimation and disturbance rejection by feedforward approach.

In the hard disk drive control, it is shown that multirate controllers have advantages both in the feedback performance [2, 4, 5] and the feedforward performance [2, 6, 7]. However, this paper makes first attempt to apply the multirate control to vibration suppression control and repetitive disturbance rejection control.

2 Discretization of controller based on multirate input control

In this section, novel discretization method of an analog controller is proposed for the system with longer sampling period $(T_u < T_y)$ base on the multirate input control. The proposed method is applied to vibration suppression controller in 4.1. For the restriction of $T_u < T_y$, the flame period T_f is defined as $T_f = T_y$, and the dynamics of the controller is described by T_f.

In the proposed multirate scheme, the plant input is changed N times during $T_y (= T_f)$ as shown in Fig.2. An integer M is selected so as to $M \triangleq N/n$ becomes an integer, where N is the input multiplicity and n is the plant order.

For simplification, the continuous-time plant is assumed to be SISO system in this paper. The proposed methods, however, can be extended to deal with the MIMO system by the same way as [1].

2.1 Plant Discretization by Multirate Sampling

Consider the continuous-time plant described by

$$\dot{x}(t) = A_c x(t) + b_c u(t) \; , \quad y(t) = c_c x(t). \tag{1}$$

The discrete-time plant discretized by the multirate sampling control (Fig.2) becomes

$$x[i+1] = Ax[i] + Bu[i] \; , \quad y[i] = Cx[i], \tag{2}$$

where $x[i] = x(iT)$, and matrices A, B, C and vectors u are given by

$$\left[\begin{array}{c|c} A & B \\ \hline C & O \end{array} \right] \triangleq \left[\begin{array}{c|ccc} e^{A_c T_f} & b_1 & \cdots & b_N \\ \hline c_c & 0 & \cdots & 0 \end{array} \right], \tag{3}$$

$$b_j \triangleq \int_{(1-\mu_j)T_f}^{(1-\mu_{(j-1)})T_f} e^{A_c \tau} b_c d\tau \; , \quad u \triangleq [u_1, \cdots, u_N]^T, \tag{4}$$

$$0 = \mu_0 < \mu_1 < \mu_2 < ... < \mu_N = 1. \tag{5}$$

The inter-sample plant state at $t = (i + \nu_k)T_f$ is represented by

$$\tilde{x}[i] = \tilde{A}x[i] + \tilde{B}u[i], \tag{6}$$

$$\left[\begin{array}{c|c} \tilde{A} & \tilde{B} \end{array} \right] \triangleq \left[\begin{array}{c|ccc} \tilde{A}_1 & \tilde{b}_{11} & \cdots & \tilde{b}_{1N} \\ \vdots & \vdots & & \vdots \\ \tilde{A}_M & \tilde{b}_{M1} & \cdots & \tilde{b}_{MN} \end{array} \right], \tag{7}$$

$$\tilde{A}_k \triangleq e^{A_c \nu_k T_f}, \; \tilde{x} \triangleq [x_1, \cdots, x_M]^T, \tag{8}$$

$$x_k[i] = x[i + \nu_k] = x((i + \nu_k)T_f), \tag{9}$$

$$\tilde{b}_{kj} \triangleq \left\{ \begin{array}{ll} \mu_j < \nu_k : & \int_{(\nu_k - \mu_j)T_f}^{(\nu_k - \mu_{(j-1)})T_f} e^{A_c \tau} b_c d\tau \\ \mu_{(j-1)} < \nu_k \leq \mu_j : & \int_0^{(\nu_k - \mu_{(j-1)})T_f} e^{A_c \tau} b_c d\tau \\ \nu_k \leq \mu_{(j-1)} : & 0 \end{array} \right. ,$$

$$0 < \nu_1 < \nu_2 < ... < \nu_M = 1. \tag{10}$$

where $\mu_j(j = 0, 1, \cdots, N)$ and $\nu_k(k = 1, \cdots, M)$ are the parameters for multirate sampling as shown in Fig.2. If T_f is divided at same intervals, $\mu_j = j/N, \nu_k = k/M$.

2.2 Design of continuous-time controller

In this section, the continuous-time controller is designed based on the regulator and the disturbance observer.

Consider the continuous-time plant model described by

$$\dot{x}_p(t) = A_{cp} x_p(t) + b_{cp}(u(t) - d(t)) \tag{11}$$

$$y(t) = c_{cp} x_p(t), \tag{12}$$

where $d(t)$ is the disturbance input. Let the disturbance model be

$$\dot{x}_d(t) = A_{cd} x_d(t) \; , \; d(t) = c_{cd} x_d(t). \tag{13}$$

For example, the step type disturbance can be modeled by $A_{cd} = 0, c_{cd} = 1$. The continuous-time augmented system consisting of (11) and (13) is represented by

$$\dot{x}(t) = A_c x(t) + b_c u(t) \tag{14}$$

$$y(t) = c_c x(t), \tag{15}$$

$$A_c \triangleq \left[\begin{array}{cc} A_{cp} & -b_{cp} c_{cd} \\ O & A_{cd} \end{array} \right], b_c \triangleq \left[\begin{array}{c} b_{cp} \\ 0 \end{array} \right], x \triangleq \left[\begin{array}{c} x_p \\ x_d \end{array} \right],$$

$$c_c \triangleq [c_{cp}, 0].$$

For the plant (14), the continuous-time observer is designed from the Gopinath's method by

$$\dot{v}(t) = \hat{A}_c \hat{v}(t) + \hat{b}_c y(t) + \hat{J}_c u(t) \tag{16}$$

$$\hat{x}(t) = \hat{C}_c \hat{v}(t) + \hat{d}_c y(t). \tag{17}$$

In order to regulate the plant state and reject the disturbance, the continuous-time regulator is designed by

$$u(t) = f_{cp} \hat{x}_p(t) + c_{cd} \hat{x}_d(t) = f_c \hat{x}(t), \tag{18}$$

$$f_c \triangleq [f_{cp}, c_{cd}]. \tag{19}$$

Letting e_v be the estimation errors of the observer ($e_v = \hat{v} - v$), the following equation is obtained.

$$\hat{x}(t) = x(t) + \hat{C} e_v(t). \tag{20}$$

From the above equations, the closed-loop system is represented by

$$
\begin{bmatrix} \dot{\boldsymbol{x}}_p(t) \\ \dot{\boldsymbol{x}}_d(t) \\ \dot{\boldsymbol{e}}_v(t) \end{bmatrix} = \begin{bmatrix} \boldsymbol{A}_{Fcp} & \boldsymbol{O} & \boldsymbol{b}_{cp}\boldsymbol{f}_c\hat{\boldsymbol{C}}_c \\ \boldsymbol{O} & \boldsymbol{A}_d & \boldsymbol{O} \\ \boldsymbol{O} & \boldsymbol{O} & \hat{\boldsymbol{A}}_c \end{bmatrix} \begin{bmatrix} \boldsymbol{x}_p(t) \\ \boldsymbol{x}_d(t) \\ \boldsymbol{e}_v(t) \end{bmatrix}, \quad (21)
$$

where $\boldsymbol{A}_{Fcp} \triangleq \boldsymbol{A}_{cp} + \boldsymbol{b}_{cp}\boldsymbol{f}_{cp}$. The transitions of the states $\boldsymbol{x}_p, \boldsymbol{x}_d$ from $t = iT_f$ to $t = (i + \nu_k)T_f$ are represented by

$$
\begin{bmatrix} \boldsymbol{x}_p[i + \nu_k] \\ \boldsymbol{x}_d[i + \nu_k] \\ \boldsymbol{e}_v[i + 1] \end{bmatrix} = \qquad\qquad (22)
$$

$$
\begin{bmatrix} e^{\boldsymbol{A}_{Fcp}\nu_k T_f} & \boldsymbol{O} & * \\ \boldsymbol{O} & e^{\boldsymbol{A}_d\nu_k T_f} & \boldsymbol{O} \\ \boldsymbol{O} & \boldsymbol{O} & e^{\hat{\boldsymbol{A}}_c T_f} \end{bmatrix} \begin{bmatrix} \boldsymbol{x}_p[i] \\ \boldsymbol{x}_d[i] \\ \boldsymbol{e}_v[i] \end{bmatrix}. \ (23)
$$

2.3 Discretization of the controller by multirate input control

In this section, the digital controller is obtained from the continuous-time controller designed in 2.2 using multirate input control.

Discretizing (14) by the multirate sampling control, the inter-sample plant state at $t = (i+\nu_k)T_f$ can be calculated from the kth row of (6) by

$$
\boldsymbol{x}[i + \nu_k] = \tilde{\boldsymbol{A}}_k\boldsymbol{x}[i] + \tilde{\boldsymbol{B}}_k\boldsymbol{u}[i] \qquad (24)
$$

$$
\tilde{\boldsymbol{A}}_k = \begin{bmatrix} \tilde{\boldsymbol{A}}_{pk} & \tilde{\boldsymbol{A}}_{pdk} \\ \boldsymbol{O} & \tilde{\boldsymbol{A}}_{dk} \end{bmatrix}, \tilde{\boldsymbol{B}}_k = \begin{bmatrix} \tilde{\boldsymbol{B}}_{pk} \\ \boldsymbol{O} \end{bmatrix}.
$$

For the plant (14) discretized by (2), the discrete-time observer on the sampling points is obtained by

$$
\hat{\boldsymbol{v}}[i + 1] = \hat{\boldsymbol{A}}\hat{\boldsymbol{v}}[i] + \hat{\boldsymbol{b}}y[i] + \hat{\boldsymbol{J}}\boldsymbol{u}[i] \qquad (25)
$$

$$
\hat{\boldsymbol{x}}[i] = \hat{\boldsymbol{C}}\hat{\boldsymbol{v}}[i] + \hat{\boldsymbol{d}}y[i]. \qquad (26)
$$

As shown in Fig.3, let the feedback control law be

$$
\boldsymbol{u}[i] = \boldsymbol{F}_p\hat{\boldsymbol{x}}_p[i] + \boldsymbol{F}_d\hat{\boldsymbol{x}}_d[i] = \boldsymbol{F}\hat{\boldsymbol{x}}[i], \qquad (27)
$$

where $\boldsymbol{F} \triangleq [\boldsymbol{F}_p, \boldsymbol{F}_d]$. From (24) to (20), the closed-loop system is represented by

$$
\begin{bmatrix} \boldsymbol{x}_p[i + \nu_k] \\ \boldsymbol{x}_d[i + \nu_k] \\ \boldsymbol{e}_v[i + 1] \end{bmatrix} = \qquad\qquad (28)
$$

$$
\begin{bmatrix} \tilde{\boldsymbol{A}}_{pk} + \tilde{\boldsymbol{B}}_{pk}\boldsymbol{F}_p & \tilde{\boldsymbol{A}}_{pdk} + \tilde{\boldsymbol{B}}_{pk}\boldsymbol{F}_d & \tilde{\boldsymbol{B}}_{pk}\boldsymbol{F}\hat{\boldsymbol{C}} \\ \boldsymbol{O} & \tilde{\boldsymbol{A}}_{dk} & \boldsymbol{O} \\ \boldsymbol{O} & \boldsymbol{O} & \hat{\boldsymbol{A}} \end{bmatrix} \begin{bmatrix} \boldsymbol{x}_p[i] \\ \boldsymbol{x}_d[i] \\ \boldsymbol{e}_v[i] \end{bmatrix}.
$$

Comparing (22) and (28), if the following conditions are satisfied, the plant state ($\boldsymbol{x}_p$) of the digitally controlled system completely matches that of the original continuous-time system at M inter-sample points on $t = (i + \nu_k)T_f$.

$$
\tilde{\boldsymbol{A}}_{pk} + \tilde{\boldsymbol{B}}_{pk}\boldsymbol{F}_p = e^{\boldsymbol{A}_{Fcp}\nu_k T_f}, \qquad (29)
$$

$$
\tilde{\boldsymbol{A}}_{pdk} + \tilde{\boldsymbol{B}}_{pk}\boldsymbol{F}_d = \boldsymbol{O}, \qquad (30)
$$

$$
\boldsymbol{e}_v[i] = \boldsymbol{O}. \qquad (31)
$$

The simultaneous equations of (29) and (30) for all $k(= 1, \cdots, M)$ become

$$
\tilde{\boldsymbol{A}}_p + \tilde{\boldsymbol{B}}_p\boldsymbol{F}_p = \boldsymbol{E}, \quad \tilde{\boldsymbol{A}}_{pd} + \tilde{\boldsymbol{B}}_p\boldsymbol{F}_d = \boldsymbol{O} \qquad (32)
$$

$$
\begin{bmatrix} \tilde{\boldsymbol{A}}_p & | & \tilde{\boldsymbol{A}}_{pd} & | & \tilde{\boldsymbol{B}}_p & | & \boldsymbol{E} \end{bmatrix}
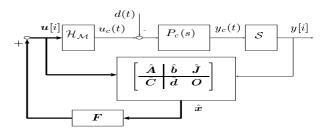$$

Fig. 3: Multirate control with disturbance observer.

$$
\triangleq \begin{bmatrix} \tilde{\boldsymbol{A}}_{p1} & \tilde{\boldsymbol{A}}_{pd1} & \tilde{\boldsymbol{B}}_{p1} & e^{\boldsymbol{A}_{Fcp}\nu_1 T_f} \\ \vdots & \vdots & \vdots & \vdots \\ \tilde{\boldsymbol{A}}_{pM} & \tilde{\boldsymbol{A}}_{pdM} & \tilde{\boldsymbol{B}}_{pM} & e^{\boldsymbol{A}_{Fcp}\nu_M T_f} \end{bmatrix}.
$$

Because non-singularity of the matrix $\tilde{\boldsymbol{B}}_p$ can be assured [2, 8], $\boldsymbol{F}_p$ and $\boldsymbol{F}_d$ are obtained by

$$
\boldsymbol{F}_p = \tilde{\boldsymbol{B}}_p^{-1}(\boldsymbol{E} - \tilde{\boldsymbol{A}}_{pd}), \quad \boldsymbol{F}_d = -\tilde{\boldsymbol{B}}_p^{-1}\tilde{\boldsymbol{A}}_{pd}. \qquad (33)
$$

Moreover, [1] proposed the discretization for observer based on multirate output control, where the plant output is detected more frequently than the control period ($T_y < T_u$). However, in this paper, discrete-time observer (25) is simply obtained, so that the eigenvalues of $\hat{\boldsymbol{A}}$ become identical to those of $e^{\hat{\boldsymbol{A}}_c T_f}$, because the plant is assumed to have longer sampling period ($T_y > T_u$).

Substituting (25) for (27), the feedback type controller is obtained by

$$
\begin{bmatrix} \hat{\boldsymbol{v}}[i + 1] \\ \boldsymbol{u}[i] \end{bmatrix} = \begin{bmatrix} \hat{\boldsymbol{A}} + \hat{\boldsymbol{J}}\boldsymbol{F}\hat{\boldsymbol{C}} & \hat{\boldsymbol{b}} + \hat{\boldsymbol{J}}\boldsymbol{F}\hat{\boldsymbol{d}} \\ \boldsymbol{F}\hat{\boldsymbol{C}} & \boldsymbol{F}\hat{\boldsymbol{d}} \end{bmatrix} \begin{bmatrix} \hat{\boldsymbol{v}}[i] \\ y[i] \end{bmatrix}. \ (34)
$$

2.4 Initial value compensation

In this section, the initial value of the controller (34) is considered in order to eliminate the estimation error of the observer and satisfy (31). From (26), if $\boldsymbol{x}[0]$ is known, the initial value of controller should be set by

$$
\hat{\boldsymbol{C}}\hat{\boldsymbol{v}}[0] = \boldsymbol{x}[0] - \hat{\boldsymbol{d}}y[0]. \qquad (35)
$$

By this compensation, it is possible to prevent the overshoot of the step (or initial value) response because the plant state converges only by the mode of the regulator. Therefore, $\boldsymbol{f}_{cp}$ should be designed to assign the eigenvalues of $\boldsymbol{A}_{Fcp}$ to the zero (or small) overshoot region.

3 Repetitive control based on multirate input control

In this section, two multirate repetitive controllers are proposed, which are 1) feedback approach based on internal model principle and 2) feedforward disturbance rejection approach based on the open-loop estimation.

3.1 Feedback repetitive control

The periodic disturbance of $T_0 \triangleq 2\pi/\omega_0$ can be represented by

$$
d(t) = a_0 + \sum_{k=1}^{\infty} a_k \cos k\omega_0 t + b_k \sin k\omega_0 t. \qquad (36)
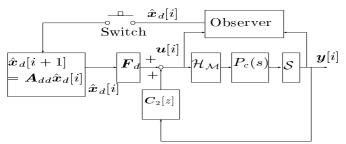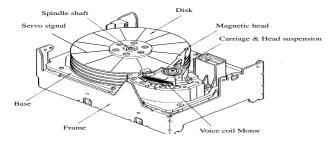$$

Fig. 4: Feedforwad repetitive control

Fig. 5: Hard disk drive.

Letting the disturbance model (13) be (36), the repetitive feedback controller is obtained by (34), which has internal model $s^2 + (k\omega_0)^2$.

From (28) and (30), the influence from disturbance $\boldsymbol{x}_d[i]$ to the inter-sample state $\boldsymbol{x}_p[i+\nu_k]$ becomes zero at $t = (i+\nu_k)T_f$. Moreover, $\boldsymbol{x}_p[i]$ and $\boldsymbol{e}_v[i]$ converge to zero at the rate of the eigenvalues of $\tilde{\boldsymbol{A}}_{pM} + \tilde{\boldsymbol{B}}_{pM}\boldsymbol{F}_p$ and $\hat{\boldsymbol{A}}$ (the poles of the regulator and observer). Therefore, the repetitive disturbance is perfectly rejected ($\boldsymbol{x}_p[i+\nu_k] = 0$) at M inter-sample points in the steady state.

3.2 Feedforward repetitive control

The repetitive feedback control based on the internal model principle has disadvantages that the closed-loop characteristics become worse and difficult to assure stability robustness [3]. Therefore, in this section, novel repetitive controller based on the open-loop estimation and feedforward disturbance rejection are proposed as shown in Fig.4

The repetitive disturbance is estimated by the open-loop disturbance observer. When the estimation converges to the steady state, the switch turns on at $t = t_0$. After that, the switch turns off immediately. The repetitive disturbance is calculated from the initial value $\hat{\boldsymbol{x}}_d[t_0]$ by

$$\hat{\boldsymbol{x}}_d[i+1] = \boldsymbol{A}_{dd}\hat{\boldsymbol{x}}_d[i], \qquad (37)$$

where $\boldsymbol{A}_{dd} = e^{\boldsymbol{A}_{cd}T_f}$. Because the disturbance feedforward $\boldsymbol{F}_d$ is obtained by (33), the perfect disturbance rejection is achieved at M inter-sample points. The advantage of this approach is that the stability robustness can be guaranteed easily only by the conventional feedback controller $\boldsymbol{C}_2[z]$.
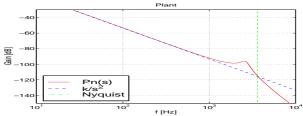

Fig. 6: Frequency responses of plant.

Table 1: Plant's parameters.

Amplifier gain	K_a	1.996	A/V
Force constant	K_f	2.95	N/A
Mass	M_p	6.983	g
Track pitch	T_p	3.608	μm/trk
Sampling time	T_s	138.54	μsec
Input multiplicity	N	4	
Mechanical resonance	ω_{1n}	$2\pi \times 2.7 \times 10^3$	rad/sec
Damping	ζ_{1n}	0.1	

4 Applications to HDD

In the head-positioning control of hard disk drives (Fig.5), the control strategy is divided into three modes; seeking mode, settling mode, and following mode. In the seeking mode, the head is moved to the desired track as fast as possible. Next, the head is settled to the track without overshoot in the settling mode. After that, the head need to be positioned on the desired track while the information is read or written. In the following mode, the head is positioned finely on the desired track under the vibrations generated by the disk rotation and disturbance [9].

In this section, the proposed feedback controllers are applied to the settling and following modes. While servo signals are detected at a constant period about 100 [μs], the control input can be changed 2~4 times between one sampling period in the recent hardware [6, 7]. Therefore, the proposed approaches are applicable.

4.1 Vibration suppression control based on multirate input control
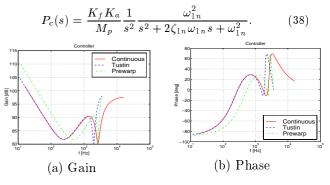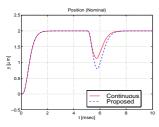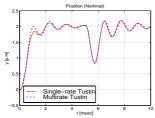
Let the nominal model of this plant be

$$P_c(s) = \frac{K_f K_a}{M_p} \frac{1}{s^2} \frac{\omega_{1n}^2}{s^2 + 2\zeta_{1n}\omega_{1n}s + \omega_{1n}^2}. \qquad (38)$$

(a) Gain   (b) Phase

Fig. 7: Frequency responses of controller

(a) Continuous-time and proposed controllers

(b) Tustin transformations

Fig. 8: Time responses

(a) Continuous-time

(b) Proposed controller
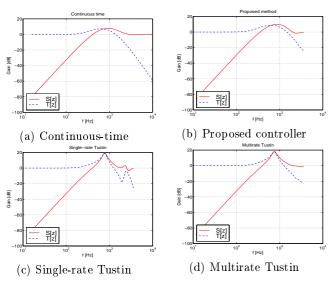
(c) Single-rate Tustin

(d) Multirate Tustin

Fig. 9: Frequency responses $S[z], T[z]$

The parameters of this plant are shown in Table 1. This model is obtained from the experimental setup of 3.5-in hard disk drive [2]. As shown in Fig.6, the actual plant has the first mechanical resonance mode around 2.7 [kHz], and its variation range is $\pm$ 500 [Hz]. The Nyquist frequency (3.6 [kHz]) is close to this resonance mode. Therefore, it is very difficult to suppress the vibration in the conventional single-rate controller.

Continuous-time controller is designed by regulator and disturbance observer, in which the disturbance is modeled by the step type function $d(s) = 1/s$, the poles of the regulator are set to $(s + \omega_c)^4$, and those of the observer are set to $(s + \omega_c)^2(s^2 + 2\zeta_1\omega_{1n}s + \omega_{1n}^2)$. As shown in Fig.7, this controller has notch characteristic at the resonance
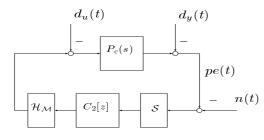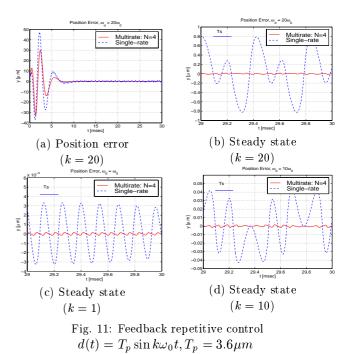

Fig. 10: Following mode.

(a) Position error
($k = 20$)

(b) Steady state
($k = 20$)

(c) Steady state
($k = 1$)

(d) Steady state
($k = 10$)

Fig. 11: Feedback repetitive control
$d(t) = T_p \sin k\omega_0 t, T_p = 3.6\mu m$

frequency. The parameter ω_c is tuned so that the bandwidth of the closed-loop system is set as high as possible, and stabilize the $\pm$ 1 [kHz] resonance variation. Fig.7 also shows that the Tustin transformation has large approximation error because the resonance mode is close to the Nyquist frequency.

Simulated results are shown in Fig.8 and Fig.9, which indicate that the proposed method has better performance than the Tustin transformations. "Multirate Tustin" is composed of the digital controller discretized by Tustin transformation on T_y/N and the interpolator which has an up-sampler and a zero-order-hold. While the responses of the Tustin transformations are oscillated, that of the proposed method has no vibration.

4.2 Repetitive control based on multirate input control

In this section, the proposed multirate repetitive controllers are applied to the following mode. The block diagram of the following mode is shown in Fig.10. The disturbance $d_y(t)$ represents the vibration of the track generated by the disk rotation, which is called track runout. The objective of this mode is to make the position error $pe(t)$ zero. $n(t)$ and $d_u(t)$ represent the measurement noise and acceleration disturbance, respectively.

In the following mode, two kinds of disturbance should be considered; repeatable and non-repeatable runout. Repeatable runout (RRO) is synchronous with the disk rotation, and non-repeatable runout (NRRO) is not synchronous. In this paper, the RRO is perfectly rejected by the proposed repetitive controllers at M inter-sample points.

For simplification, the plant is modeled by

$$P_c(s) = \frac{K_f K_a}{M_p} \frac{1}{s^2}, \tag{39}$$
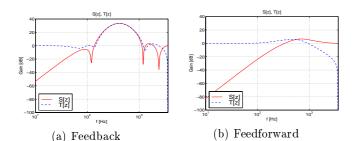
(a) Feedback (b) Feedforward

Fig. 12: Frequency responses $S[z], T[z]$

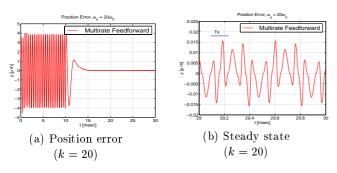(a) Position error (b) Steady state
$(k = 20)$ $(k = 20)$

Fig. 13: Feedforward repetitive control

and RRO are considered at 1st, 10th, and 20th order.

$$d(t) = \sum_{k=1,10,20} a_k \cos k\omega_0 t + b_k \sin k\omega_0 t, \qquad (40)$$

where $\omega_0 = 2\pi 120[\mathrm{rad/sec}]$. Fig.11 shows the simulated results of the proposed repetitive feedback control under the $120k$ [Hz] sinusoidal runout added from $t = 0$, which amplitude is 1 [trk] $= 3.6[\mu\mathrm{m}]$. Although the transient position errors are large, the position errors become zero at sampling point in the steady state as shown in Fig.11(a), because the feedback controllers have the internal models of the RRO. However, Fig.11(b) $\sim$ (c) show that the inter-sample responses have the tracking errors even in the steady state. It is shown that the errors of the plant position and velocity become zero at every $T_y/2$ by the proposed controllers[1]. Moreover, the inter-sample position errors of the proposed multirate method are much smaller than those of the single-rate controller. Especially, in the high frequency region ($k = 20$), the position error is much improved by the proposed multirate control, because the single-rate controller has large error (0.8 [μm] = 22 %).

However, Fig.12(a) indicates the disadvantages of the feedback repetitive controller, where the closed-loop characteristics become worse and difficult to assure stability robustness. On the other hand, in the proposed feedforward repetitive control, the closed-loop characteristics is dependent only on $C_2[z]$ in Fig.4 as shown in Fig.12(b).

Simulated results of the feedforward repetitive control are shown in Fig.13. The switch turns on at just $t_0 = 10[\mathrm{ms}]$. After that, the repetitive disturbance is perfectly rejected at M inter-sample points in steady state.

---

[1] In the proposed method, the perfect disturbance rejection is assured $M(= N/n_p = 4/2 = 2)$ times during T_y.

5 Conclusion

In this paper, the digital control systems which have hardware restrictions of $T_u < T_y$ are assumed, novel multirate feedback controllers are proposed, which achieve vibration suppression and disturbance rejection in the semi-Nyquist frequency region.

Furthermore, the proposed methods are applied to the settling and following modes of the hard disk drive. The advantages of these approaches are demonstrated by the simulations. The proposed methods can be extended to the plants with time delay [10].

The future works are 1) improvements of the original analog controller for vibration suppression and 2) experimental evaluations of the proposed methods.

Finally, the authors would like to note that part of this research is carried out with a subsidy of the Scientific Research Fund of the Ministry of Education.

References

[1] H. Fujimoto, A. Kawamura, and M. Tomizuka, "Generalized digital redesign method for linear feedback system based on N-delay control," *IEEE/ASME Trans. Mechatronics*, vol. 4, no. 2, pp. 101–109, 1999.

[2] H. Fujimoto, Y. Hori, T. Yamaguchi, and S. Nakagawa, "Proposal of perfect tracking and perfect disturbance rejection control by multirate sampling and applications to hard disk drive control," in *Conf. Decision Contr.*, pp. 5277–5282, December 1999.

[3] C. Smith, K. Takeuchi, and M. Tomizuka, "Cost effective repetitive controllers for data storage devices," in *14th IFAC World Congress*, vol. B, pp. 407–412, July 1999.

[4] W.-W. Chiang, "Multirate state-space digital controller for sector servo systems," in *Conf. Decision Contr.*, pp. 1902–1907, 1990.

[5] A. M. Phillips and M. Tomizuka, "Multirate estimation and control under time-varying data sampling with application to information storage devices," in *Amer. Control Conf.*, pp. 4151–4155, 1995.

[6] S. Takakura, "Design of the tracking system using N-Delay two-degree-of-freedom control and its application to hard disk drives," in *IEEE Conf. Control Applications*, pp. 170–175, August 1999.

[7] M. Kobayashi, T. Yamaguchi, I. Oshimi, Y. Soyama, Y. Hara, and H. Hirai, "Multirate zero phase error feedforward control for magnetic disk drives," in *JSME, IIP '98*, pp. 21–22, August 1998. (in Japanese).

[8] M. Araki and T. Hagiwara, "Pole assignment by multirate-data output feedback," *Int. J. Control*, vol. 44, no. 6, pp. 1661–1673, 1986.

[9] T. Yamaguchi, H. Numasato, and H. Hirai, "A mode-switching control for motion control and its application to disk drives: Design of optimal mode-switching conditions," *IEEE/ASME Trans. Mechatronics*, vol. 3, no. 3, pp. 202–209, 1998.

[10] H. Fujimoto, Y. Hori, T. Yamaguchi, and S. Nakagawa, "Seeking control of hard disk drives by perfect tracking using multirate sampling control," in *IEE of Japan, JIASC '99*, vol. 3, pp. 535–540, August 1999. (in Japanese).